Reaction of Chloromethyl Radical with Dioxygen: Formation of the Chloromethylperoxy Radical and Its Photodissociation in Solid Argon

Mingfei Zhou,* Renhu Ma, Dongmei Yuan, and Mohua Chen

Department of Chemistry, Shanghai Key Laboratory of Molecular Catalysts and Innovative Materials, Advanced Materials Laboratory, Fudan University, Shanghai 200433, P. R. China

Received: November 2, 2008; Revised Manuscript Received: January 8, 2009

The reaction of chloromethyl radical with molecular oxygen in solid argon has been studied using matrix isolation infrared absorption spectroscopy. The chloromethyl radical was produced via codeposition of chloromethane with high frequency discharged argon atoms. The chloromethyl radical reacted with dioxygen spontaneously on annealing to form the chloromethylperoxy radical, which was characterized on the basis of isotopic splitting (Cl and O) as well as quantum chemical calculations. The chloromethylperoxy radical dissociated to give the weakly bound $ClCO-H_2O$ complex under UV light irradiation. The calculations predicted that the $ClCO-H_2O$ complex was produced by hydrogen atom transfer from a CHCl(O)−OH intermediate.

Introduction

Simple organic peroxy radicals such as alkylperoxy radicals are important intermediate species in many chemical processes including combustion and atmospheric chemistry. The spectra and structures of organic peroxy radicals, and the kinetic and mechanism of reactions associated with such radicals have been extensively studied both experimentally and theoretically.[1,2]

Chloromethane is the most important natural halogenated alkane released into atmosphere. The atmospheric oxidation of chloromethane is initiated by reaction with OH in forming the chloromethyl radical, CH_2Cl, which rapidly reacts with dioxygen to yield the chloromethylperoxy radical, CH_2ClO_2. The chloromethylperoxy radical could further react with itself and with various atmospheric constituents such as HO_2, NO, and NO_2. The chloromethylperoxy radicals were produced via photolysis of $Cl_2/CH_3Cl/O_2$ mixtures in the gas phase, and the UV absorption spectra were obtained.[3,4] The kinetics of the reactions of chloromethylperoxy radical with itself and with HO_2 were studied, and the reaction rate constants were measured.[3−5] The mechanism of the reaction of chloromethylperoxy radical with HO_2 was investigated using Fourier transform infrared spectroscopy.[6] Both the CH_2ClOOH and HC(O)Cl molecules were identified as the reaction product. The chloromethylperoxy radical and HO_2 reaction was also theoretically studied to elucidate the observed reaction mechanism.[7,8]

Matrix isolation is an effective technique to trap peroxy radicals for spectroscopic study. The infrared absorption spectra of some simple peroxy radicals such as CH_3OO, CF_3OO, C_2H_3OO, and HC(O)OO isolated in noble gas matrixes were reported.[9−16] These radicals were produced either via the initial production of an organic radical with subsequent reaction with oxygen or via vacuum flash pyrolysis of thermally labile precursors. To our knowledge, no experimental IR data of chloromethylperoxy radical have been reported to date. Here we present a combined matrix isolation infrared absorption spectroscopic and theoretical study of the reaction between chloromethyl radical and molecular oxygen in solid argon. The infrared absorption spectrum of the resulting chloromethylperoxy radical is obtained and assigned. In addition, the photodissociation products from chloromethylperoxy radical are also reported.

Experimental and Computational Methods

The chloromethyl radical was prepared by high frequency discharge. The experimental setup for matrix isolation Fourier transform infrared spectroscopic investigation has been described in detail previously.[17] Briefly, one pure argon gas stream was subjected to discharge from a high-frequency generator (Tesla coil, alternating voltage ranging from 0 to 9 kV and frequency ranging from 10 to 15 kHz). The tip of the Tesla coil was connected to a copper cap on one end of a quartz tube extending into the vacuum chamber. The other end of the quartz tube was connected to a copper tube with ground potential. Discharge takes place between the cap and the copper tube. The quartz tube is about 20 mm long with an internal diameter of 3 mm. The resulting beam is mixed with another gas stream containing CH_3Cl/Ar or CH_3Cl/O_2/Ar samples outside the discharge region, followed by codeposition on the surface of a CsI window cooled normally to 4 K by means of a closed-cycle helium refrigerator. In general, matrix samples were deposited for 1 h at a rate of approximately 5 mmol/h for each stream. The infrared absorption spectra of the resulting samples were recorded on a Bruker Vertex 80v spectrometer at 0.5 cm^{-1} resolution between 4000 and 450 cm^{-1} using a DTGS detector. After the infrared spectrum of the initial deposit had been recorded, the sample was annealed to different temperatures and cooled back to 4 K for spectral acquisition. Selected samples were also subjected to broadband irradiation using a high pressure mercury arc lamp (250−580 nm) with glass filters. The CH_3Cl/O_2/Ar (1:5:1000−1:5:2000) mixtures were prepared in a stainless steel vacuum line using standard manometric technique. CH_3Cl (Aldrich, >99.5%), O_2 (Shanghai BOC, >99.5%), and $^{18}O_2$ (Cambridge Isotope Laboratories, 99%) were used without purification in different experiments.

Quantum chemical calculations were performed using the Gaussian 03 program.[18] The three-parameter hybrid functional according to Becke with additional correlation corrections from Lee, Yang, and Parr (B3LYP) was utilized.[19] The 6−311++G**

* Corresponding author. E-mail: mfzhou@fudan.edu.cn.

10.1021/jp809683n CCC: $40.75
Published on Web 02/18/2009

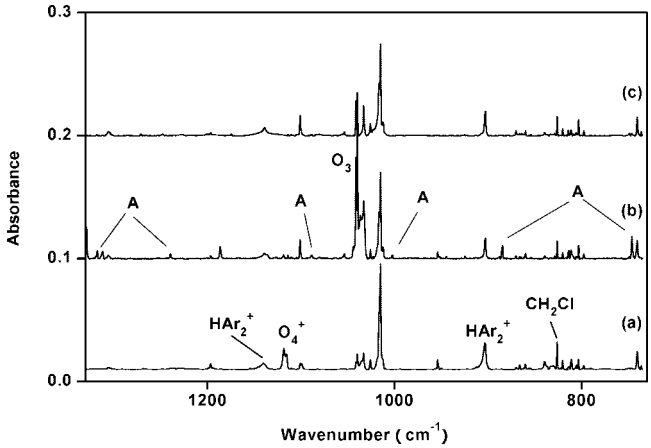

Figure 1. Infrared spectra in the 1330−730 cm^{-1} region from codeposition of 0.1% CH_3Cl/0.5% O_2/Ar with high frequency discharged Ar: (a) after 1 h of sample deposition at 4 K, (b) after 28 K annealing, and (c) after 15 min of broadband irradiation ($250 < \lambda < 580$ nm).

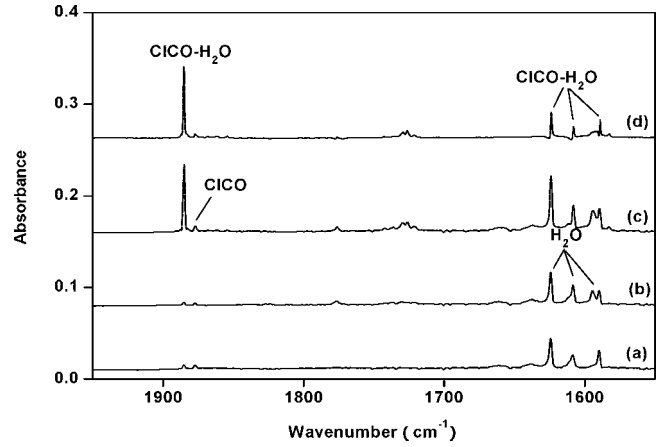

Figure 2. Infrared spectra in the 1950−1550 cm^{-1} region from codeposition of 0.1% CH_3Cl/0.5% O_2 /Ar with high frequency discharged Ar: (a) after 1 h of sample deposition at 4 K, (b) after 28 K annealing, (c) after 15 min of broadband irradiation ($250 < \lambda < 580$ nm), and (d) spectrum c minus spectrum b.

basis set was used for the H, C, O, and Cl atoms.[20] The geometries were fully optimized; the harmonic vibrational frequencies were calculated, and zero-point vibrational energies (ZPVE) were derived. Transition state optimizations were done with the synchronous transit-guided quasi-Newton (STQN) method[21] at the B3LYP/6−311++G** level. In addition, the IRC calculations were performed to verify the transition states connecting the reactant and product on the potential energy surface.

Results and Discussion

Codeposition of excited argon atoms with precursor molecules has often been used in producing free radicals in matrix isolation spectroscopic studies.[22] The present experiments found that excited argon atoms from high frequency discharge are effective in producing chloromethyl radical from the chloromethane precursor molecule. Besides the strong chloromethane absorptions, codeposition of CH_3Cl/Ar with discharged argon at 4 K resulted in fragmentation of CH_3Cl to give CH_2Cl (1390.1, 826.1 and 820.2 cm^{-1}), CHCl (803.3 and 797.5 cm^{-1}), and CCl (870.3 and 860.0 cm^{-1}).[23−25] In addition, the HAr_2^+ cation absorptions at 1139.7 and 903.1 cm^{-1} were also observed.[26] The relative intensities of these fragments depend on the power level of discharge. Generally, formation of CH_2Cl radical is favored with low power level of discharge (about 400 V alternating voltage with a frequency of 12 kHz). These fragment absorptions remained almost unchanged on subsequent annealing as well as on broadband irradiation. When the O_2/Ar sample was codeposited with high frequency discharged argon atoms, the O_4^- (953.6 cm^{-1}) and O_4^+ (1118.4 cm^{-1}) charged species were observed, while the O_3 (1039.4 cm^{-1}) neutral was produced upon sample annealing.[27] These oxygen clusters are photosensitive; they were destroyed upon broadband irradiation ($250 < \lambda < 580$ nm).

When the CH_3Cl/O_2/Ar mixture was codeposited with discharged argon, additional new absorptions were produced. The infrared absorption spectra in selected regions are shown in Figures 1 and 2, respectively. Figure 3 shows two difference spectra from the spectra of Figure 1. As can clearly be seen in Figure 1 and the difference spectra shown in Figure 3, the CH_2Cl absorptions decreased, while a group of new absorptions at 1311.9, 1239.4, 1088.2, 1002.3, 884.6, 746.2, and 741.7 cm^{-1} (labeled as A in Figure 1) were produced when the sample was

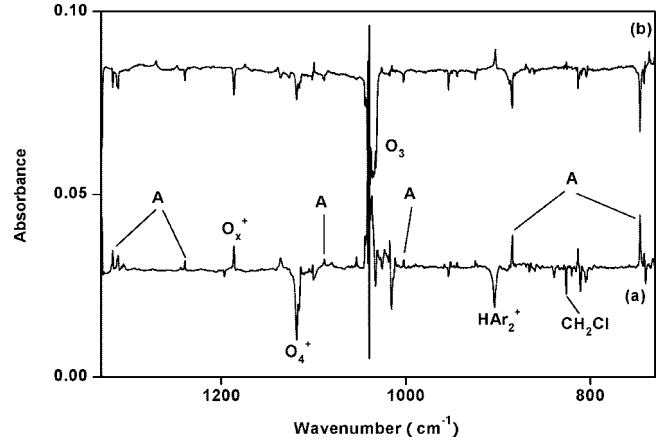

Figure 3. Difference IR spectra in the 1330−730 cm^{-1} region from codeposition of 0.1% CH_3Cl/ 0.5% O_2/Ar with high frequency discharged Ar. (a) Spectrum taken after 28 K annealing minus spectrum taken right after 1 h of sample deposition at 4 K. (b) Spectrum taken after broadband irradiation minus spectrum taken after 28 K annealing.

annealed to 28 K. The group A absorptions virtually disappeared when the sample was subjected to broadband irradiation with a high pressure mercury arc lamp, during which two new absorptions at 1885.2 and 566.8 cm^{-1} were produced. As shown in Figure 2, the bending vibration of water impurity also increased on broadband irradiation. The difference spectrum (trace d in Figure 2, spectrum after irradiation minus spectrum before irradiation) shows that the increased absorptions are slightly red-shifted (0.3 cm^{-1}) from the band positions of pure water absorptions in solid argon. Besides the above-mentioned absorptions, the HOO (3412.1, 1388.3, and 1100.7 cm^{-1}),[28] CO (2138.0 cm^{-1}) and CO_2 absorptions were also observed after sample deposition.

The experiment was repeated with the $CH_3Cl/^{18}O_2$/Ar sample. The absorptions of the CH_xCl ($x = 0, 1, 2$) fragments remain unshifted, while the oxygen clusters as well as the newly observed product absorptions are red-shifted. The band positions of the CH_xCl ($x = 0, 1, 2$) fragments and the group A absorptions together with their isotopic counterparts are listed in Table 1.

CH_2ClO_2. The group A absorptions appeared together on annealing and can be grouped together by their consistent behavior upon annealing and broadband irradiation, which

TABLE 1: Infrared Absorptions (cm^{-1}) from Codeposition of $CH_3Cl/O_2/Ar$ with High Frequency Discharged Ar at 4 K

frequency	$^{18}O_2$	assignment
1311.9	1310.0	CH_2ClO_2 CH_2 scissors
1239.4	1231.1	CH_2ClO_2 CH_2 rock
1088.2	1033.9	CH_2ClO_2 O−O stretch
1002.3	993.0	CH_2ClO_2 CH_2 rock
884.6	867.5	CH_2ClO_2 C−O stretch
746.2	745.4	$CH_2{}^{35}ClO_2$ C−Cl stretch
741.7	740.8	$CH_2{}^{37}ClO_2$ C−Cl stretch
1885.3	1838.5	$ClCO-H_2O$ C−O stretch
1623.7	1616.0	$ClCO-H_2O$ H_2O bending
566.8	561.2	$ClCO-H_2O$ C−Cl stretch
1390.1		CH_2Cl CH_2 scissors
826.2		$CH_2{}^{35}Cl\cdot$ C−Cl stretch
820.2		$CH_2{}^{37}Cl$ C−Cl stretch
803.3		$CH^{35}Cl$ C−Cl stretch
797.5		$CH^{37}Cl$ C−Cl stretch
870.3		$C^{35}Cl$
860.0		$C^{37}Cl$

suggests different vibrational modes of the same species. The spectra shown in Figures 1 and 3 clearly indicate that group A absorptions were formed at the expense of the CH_2Cl absorptions. It is reasonable to assume that the new species is formed by the reaction of CH_2Cl with O_2, and group A absorptions are assigned to the chloromethylperoxy radical. The strongest absorption of group A is located at 746.2 cm^{-1}. This absorption together with a nearby 741.7 cm^{-1} absorption both show very small oxygen isotopic shifts (~0.8 cm^{-1}). The relative IR intensities of these two absorptions match the natural isotopic abundance of chlorine (^{35}Cl:^{37}Cl = 0.76:0.24) and clearly indicate one Cl atom involvement in this mode. The band position and chlorine isotopic shift indicate that these two absorptions are due to a C−Cl stretch vibration. The 884.6 and 1088.2 cm^{-1} absorptions are quite sensitive to oxygen isotopic substitution. The 884.6 cm^{-1} absorption is the second strongest band among group A absorptions, which shifted to 867.5 cm^{-1} with $^{18}O_2$. The isotopic $^{16}O/^{18}O$ frequency ratio of 1.0197 indicates that this absorption is due to a C−O stretch vibration. The corresponding mode of the CH_3OO and CF_3OO radicals in solid argon was previously reported at 902 and 869.2 cm^{-1}, respectively.[9,14] In the experiments in which the chloromethyl radicals were allowed to react with the sample containing equal molar ratio of $^{16}O_2$ and $^{18}O_2$, this oxygen sensitive vibrational mode is identified as a well defined doublet as shown in Figure 4. The observation of doublet implies that the originating species contains only one O_2 moiety. In an analogous experiment in which a scrambled mixture of oxygen isotopes ($^{16}O_2$:$^{16}O^{18}O$:$^{18}O_2$ = 1:2:1) was used, the 884.6 cm^{-1} absorption split into four absorptions, which indicates that the two oxygen atoms are inequivalent. The much weak 1088.2 cm^{-1} absorption also exhibits a quite large oxygen isotopic shift. It shifted to 1033.9 cm^{-1} with $^{18}O_2$. The isotopic $^{16}O/^{18}O$ frequency ratio (1.0525) and band position are appropriate for an O−O stretch vibration. The O−O stretch mode of methylperoxy radical was observed at 1112 cm^{-1} with very similar isotopic $^{16}O/^{18}O$ ratio (1.053).[9] The same mode of CF_3OO was observed at 1093.0 cm^{-1} in solid argon.[14] The remaining three absorptions at 1311.9, 1239.4, and 1002.3 cm^{-1} are weak, and all exhibit no resolved chlorine isotopic shift and small oxygen isotopic shift. These absorptions are assigned to the CH_2 scissors and rocking modes of the chloromethylperoxy radical (see Table 1).

Theoretical calculations were performed on the chloromethylperoxy radical. Previous studies indicated that the analogous CH_3OO and CF_3OO radicals possess a C_s structure with a plane

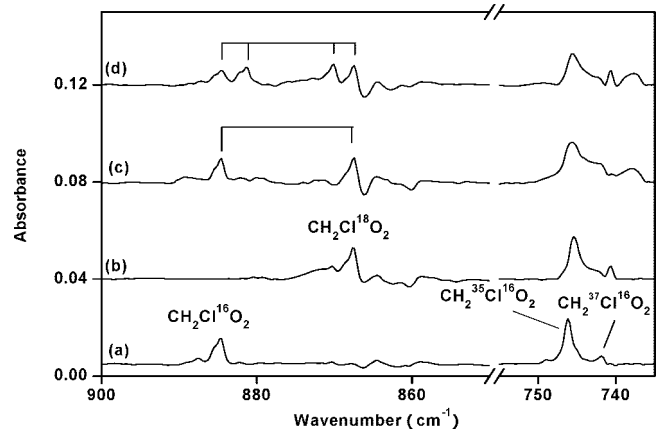

Figure 4. Difference IR spectra in the 900−850 and 755−735 cm^{-1} regions from codeposition of $CH_3Cl/O_2/Ar$ with high frequency discharged Ar at 4 K (spectrum taken after 28 K annealing minus spectrum taken right after 1 h of sample deposition). (a) 0.1% CH_3Cl/0.5% $^{16}O_2$/Ar, (b) 0.1% CH_3Cl /0.5% $^{18}O_2$/Ar, (c) 0.1% CH_3Cl/0.3% $^{18}O_2$/0.3%$^{16}O_2$/Ar, and (d) 0.1% CH_3Cl/0.15% $^{16}O_2$/ 0.3%$^{16}O^{18}O$/ 0.15% $^{18}O_2$/Ar.

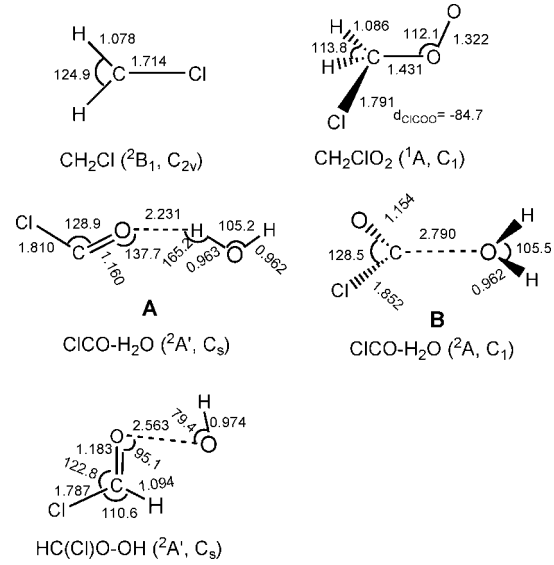

Figure 5. Optimized structures (bond lengths in angstroms; bond angles in degrees) of CH_2Cl, CH_2ClO_2, HC(Cl)O−OH, and $ClCO-H_2O$.

of symmetry.[10,14] Present DFT/B3LYP calculations on chloromethylperoxy radical predicted that a $^2A''$ state with the C_s symmetry is a stationary point. However, geometry optimization without symmetry restriction converged to a structure without symmetry, which is about 0.8 kcal/mol lower in energy than the C_s structure. The optimized structure is shown in Figure 5. The ClCO plane is roughly perpendicular to the CH_2 plane, while the terminal oxygen atom is tilted with a ClCOO dihedral angle of −84.7°. The O−O bond length of chloromethylperoxy radical was calculated to be 1.322 Å, which is quite comparable with those previously reported alkylperoxy radicals.[10,14−16]The optimized structure is in agreement with that of the previous MP2/6−31G* calculation.[6] The unpaired electron occupies on a molecular orbital which is largely O_2 antibonding π orbital in character. The calculated unpaired spin resides on the O_2 fragment with 0.26 e^- and 0.73 e^- (terminal) for the two O atoms.

The chloromethylperoxy radical without symmetry possesses 12 vibrational modes and all should be IR active. The unscaled vibrational frequencies and intensities are listed in Table 2. Six of the twelve fundamental absorptions were observed experi-

TABLE 2: Comparison between the Calculated and Observed Vibrational Frequencies and Intensities for the CH_2ClO_2 Radical

calcd		expt		
frequency	intensity[a]	frequency	intensity[b]	$CH_2Cl^{18}O_2$
100.6	1.8			
339.3	1.3			
517.8	10.3			
721.9	95.1	746.2	1.0	745.4
893.3	53.8	884.6	0.61	867.5
1014.7	9.9	1002.3	0.07	993.0
1130.9	14.8	1088.2	0.08	1119.4
1272.7	10.0	1239.4	0.07	1231.1
1346.7	34.3	1311.9	0.10	1310.0
1455.0	2.6			
3107.9	8.8			
3195.0	0.2			

[a] In km/mol. [b] Integrated intensity normalized to the most intense absorption.

mentally. Among the unobserved modes, two of them are less than 400 cm^{-1} and are out of the range of spectrometer. Two C−H stretch modes, one CH_2 scissors mode and one CH_2Cl bending mode were not observed because of low IR intensities (The antisymmetric CH_2 stretching mode at 3107.9 cm^{-1} was predicted to have comparable IR intensity with the 1014.7 cm^{-1} mode, which was observed at 1002.3 cm^{-1}, and the signal-to-noise level of spectrum above 3000 cm^{-1} is much lower than that in the 1000 cm^{-1} region; therefore, the CH_2 antisymmetric stretching mode was not able to be observed in the experiments). The calculated gas phase harmonic frequencies are slightly higher than the anharmonic vibrational frequencies observed in solid argon except for the C−Cl stretch mode, which was predicted to be more than 20 cm^{-1} lower than the observed value. As has been discussed, the C−Cl stretch vibrations are systematically underestimated with the B3LYP functional.[29] The same calculations on the CH_2Cl and CHCl molecules also predicted that the C−Cl stretch vibrations are lower than the experimentally observed values in solid argon. The predicted isotopic frequency shifts are in reasonable agreement with the experimental values, which provide strong support to the experimental assignment.

ClCO−H_2O. Two absorptions at 1885.3 and 566.8 cm^{-1} appeared on broadband irradiation at the expense of the chloromethylperoxy radical absorptions. The upper mode is due to a terminal C−O stretch vibration based upon the observed isotopic $^{16}O/^{18}O$ ratio (1.0255). The high frequency mode is 8.6 cm^{-1} above the C−O stretch mode of ClCO isolated in solid argon, whereas the low frequency mode is 3.3 cm^{-1} lower than the C−Cl stretch mode of ClCO.[30] This suggests that the 1885.3 and 566.8 cm^{-1} absorptions are due to a ClCO complex. Note that the water bending absorptions also increased on broadband irradiation. The difference spectrum shows that the increased absorptions are slightly shifted from those of pure water in solid argon. Therefore, we assign the observed absorptions to a ClCO−H_2O complex.

Theoretical calculations were also performed on the ClCO−H_2O complex. All of the possible structures were considered. Geometry optimization at the B3LYP/6−311++G** level found that two structures (labeled as **A** and **B**) are stable with respect to the separated ClCO and H_2O. The optimized structures are shown in Figure 5. Structure **A** has a planar C_s symmetry with the O atom of the ClCO fragment coordinated to one hydrogen atom of the water fragment. The ClCO−HOH distance was predicted to be 2.231 Å, which indicates a weak interaction between ClCO and H_2O. Compared to free ClCO, the C−O bond length increases by 0.0045 Å, while the C−Cl bond length decreases by 0.022Å upon H_2O coordination, which should result in a red-shift of the C−O stretch vibration (ca. 24.1 cm^{-1}) and a blue-shift of the C−Cl stretch vibration (ca. 23.3 cm^{-1}). Structure **B** was predicted to have a nonplanar geometry with the C atom of the ClCO fragment coordinated to the oxygen atom of the water subunit. The C···OH_2 distance was computed to be 2.790 Å. Structure **B** was predicted to be about 0.3 kcal/mol more stable than structure **A**. The C−O and C−Cl bond lengths in structure **B** is about 0.0016 Å shorter and 0.02 Å longer than those of free ClCO. Therefore, the computed C−O stretch vibration is 9.5 cm^{-1} blue-shifted whereas the C−Cl stretch mode is 5.5 cm^{-1} red-shifted upon water coordination in structure **B**, which are in quite good agreement with the experimentally observed shifts of 8.6 and −3.3 cm^{-1}. This indicates that the experimentally observed complex is due to structure **B**.

Reaction Mechanism. The present experiments indicate that excited argon atoms are effective in producing CH_2Cl radicals from CH_3Cl. The spectra shown in Figures 1 and 3 clearly demonstrate that annealing allows the dioxygen molecules to diffuse and react with chloromethyl radical to form the chloromethylperoxy radicals in solid argon, reaction 1, which was predicted to be exothermic by 23.5 kcal/mol. The chloromethylperoxy radical absorptions increased on annealing, which suggests that reaction 1 requires no activation energy.

Besides the chloromethyl radical, codeposition of CH_3Cl/O_2/Ar with discharged argon also produced CHCl and CCl species. No obvious absorptions that may due to products of the reactions of CHCl and CCl with dioxygen were observed. The $CHClO_2$ molecule was predicted to have a singlet ground state ($^1A'$) with a side-on bonded O_2 subunit having two strong C−Cl and CH bending vibrations at 754.9 and 1346.0 cm^{-1}.

The chloromethylperoxy radical absorptions disappeared under broadband ($250 < \lambda < 580$ nm) irradiation, during which the ClCO−H_2O complex absorptions were produced. The filtered photolysis experiments show that only the UV photons in the 250−300 nm wavelength range are responsible for the observed reaction. It appears that UV light initiates dissociation reaction 2. Most of the formed ClCO and H_2O fragments cannot escape the matrix "cage", and recombine to form the ClCO−H_2O complex.

$$CH_2Cl(^2B_1) + O_2(^3\Sigma_g^-) \rightarrow CH_2ClO_2(^2A) \quad \Delta E = -23.5 \text{ kcal/mol} \quad (1)$$

$$CH_2ClO_2 + h\nu(250 < \lambda < 300 \text{ nm}) \rightarrow ClCO{-}H_2O \quad (2)$$

Previous gas phase studies on the reactions of CH_2ClO_2 radicals with HO_2 radicals, the HCCl(O) and hydroperoxy CH_2ClOOH species were identified as the products.[6] No HC(Cl)O absorptions were observed in the present experiments, and the ClCO−H_2O complex is the major photodissociation product experimentally observed. The potential energy profiles shown in Figure 6 indicate that the dissociation reaction (2) proceeds via a CHClOOH intermediate lying 39.2 kcal/mol lower in energy than the chloromethylperoxy radical. The CHClOOH intermediate is not a hydroperoxy but is characterized to be a HC(Cl)O−OH complex (Figure 5). Geometry optimization starting on the hydroperoxy CHClOOH structure converged to the HC(Cl)O−OH complex, which indicates that the hydroperoxy structure is not a stationary point. The barrier

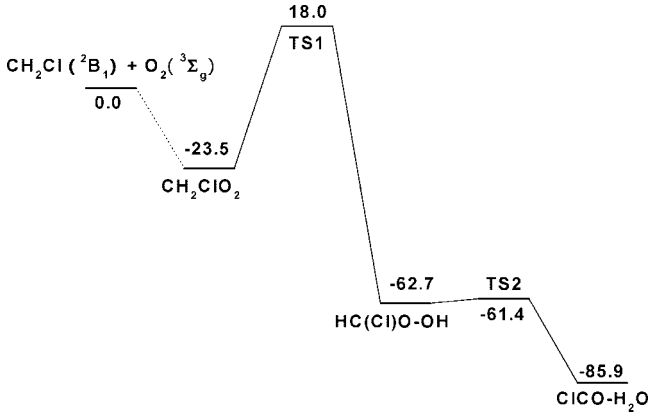

Figure 6. Potential energy profiles for the $CH_2Cl + O_2$ reaction calculated at the B3LYP/6−311++G** level of theory (values are given in kcal/mol).

from chloromethylperoxy radical to the HC(Cl)O−OH intermediate was estimated to be 41.5 kcal/mol. From the HC(Cl)O−OH intermediate, the hydrogen atom of the HC(Cl)O subunit is transferred to the OH subunit to give the $ClCO-H_2O$ complex. This process proceeds via a transition state lying only about 1.3 kcal/mol above the HC(Cl)O−OH intermediate. There is large amount of heat released during the formation of the HC(Cl)O−OH intermediate from the chloromethylpeoxy radical, the HC(Cl)O−OH intermediate could easily surmount the barrier to the more stable $ClCO-H_2O$ complex. The photon energies of UV light used in the present experiments exceed the energy barrier from the chloromethylperoxy radical to the final $ClCO-H_2O$ product. Therefore, the experimentally observed reaction is a photochemical process during which some excited electronic states may be involved.

Conclusions

The reaction of chloromethyl radical with molecular oxygen in solid argon has been studied using matrix isolation infrared absorption spectroscopy. The reaction intermediates and products were identified on the basis of isotopic IR studies as well as quantum chemical calculations. The chloromethyl radical was produced through codeposition of chloromethane with high frequency discharged argon atoms. In solid argon, the chloromethyl radical reacted with dioxygen to form the chloromethylperoxy radical spontaneously on annealing. Six of the twelve vibrational fundamentals of the chloromethylperoxy radical were observed. The chloromethylperoxy radical underwent UV photon-induced dissociation to give the weakly bound $ClCO-H_2O$ complex. The calculation results show that the $ClCO-H_2O$ complex was produced by hydrogen atom transfer from a CHCl(O)−OH intermediate on the potential energy surface.

Acknowledgment. This work is supported by NKBRSF (2007CB815203) and NNSFC (20773030) of China.

References and Notes

(1) Laufer, A. H.; Fahr, A. *Chem. Rev.* **2004**, *104*, 2813.

(2) Sharp, E. N.; Rupper, P.; Miller, T. A. *Phys. Chem. Chem. Phys.* **2008**, *10*, 3955.

(3) Dagaut, P.; Wallington, T. J.; Kurylo, M. J. *Int. J. Chem. Kinet.* **1988**, *20*, 815..

(4) Catoire, V.; Lesclaux, R.; Lightfoot, P. D. *J. Phys. Chem.* **1994**, *98*, 2889.

(5) Biggs, P.; Canosa-Mas, C. E.; Percival, C. J.; Shallcross, D. E.; Wayne, R. P *Int. J. Chem. Kinet.* **1999**, *31*, 433.

(6) Wallington, T. J.; Hurley, M. D.; Schneider, W. F. *Chem. Phys. Lett.* **1996**, *251*, 164.

(7) Hou, H.; Deng, L. Z.; Li, J. C.; Wang, B. S. *J. Phys. Chem. A* **2005**, *109*, 9299.

(8) Wei, W. M.; Zheng, R. H. *J. Mol. Struct. (THEOCHEM)* **2007**, *812*, 1.

(9) Ase, P.; Bock, W.; Snelson, A. *J. Phys. Chem.* **1986**, *90*, 2099.

(10) Nandi, S.; Blanksby, S. J.; Zhang, X.; Nimlos, M. R.; Dayton, D. C.; Ellison, G. B. *J. Phys. Chem. A* **2002**, *106*, 7547.

(11) Smardzewski, R. R.; DeMarco, R. A.; Fox, W. B. *J. Chem. Phys.* **1975**, *63*, 1083.

(12) Butler, R.; Snelson, A. *J. Phys. Chem.* **1979**, *83*, 3243.

(13) Clemitshaw, K. C.; Sodeau, J. R. *J. Phys. Chem.* **1989**, *93*, 3552.

(14) Sander, S.; Pernice, H.; Willner, H. *Chem. Eur. J.* **2000**, *6*, 3645.

(15) Yang, R. J.; Yu, L.; Jin, X.; Zhou, M. F.; Carpenter, B. K. *J. Chem. Phys.* **2005**, *122*, 014511.

(16) Yang, R. J.; Yu, L.; Zeng, A. H.; Zhou, M. F. *J. Phys. Chem. A* **2004**, *104*, 4228.

(17) Wang, G. J.; Zhou, M. F. *Int. Rev. Phys. Chem.* **2008**, *27*, 1.

(18) Frisch, M. J.; Trucks, G. W.; Schlegel, H. B.; Scuseria, G. E.; Robb, M. A.; Cheeseman, J. R.; Montgomery, J. A., Jr.; Vreven, T.; Kudin, K. N.; Burant, J. C.; Millam, J. M.; Iyengar, S. S.; Tomasi, J.; Barone, V.; Mennucci, B.; Cossi, M.; Scalmani, G.; Rega, N.; Petersson, G. A.; Nakatsuji, H.; Hada, M.; Ehara, M.; Toyota, K.; Fukuda, R.; Hasegawa, J.; Ishida, M.; Nakajima, T.; Honda, Y.; Kitao, O.; Nakai, H.; Klene, M.; Li, X.; Knox, J. E.; Hratchian, H. P.; Cross, J. B.; Adamo, C.; Jaramillo, J.; Gomperts, R.; Stratmann, R. E.; Yazyev, O.; Austin, A. J.; Cammi, R.; Pomelli, C.; Ochterski, J. W.; Ayala, P. Y.; Morokuma, K.; Voth; G. A.; Salvador, P.; Dannenberg, J. J.; Zakrzewski; V. G.; Dapprich, S.; Daniels, A. D.; Strain, M. C.; Farkas, O.; Malick, D. K.; Rabuck, A. D.; Raghavachari, K.; Foresman, J. B.; Ortiz, J. V.; Cui, Q.; Baboul, A. G.; Clifford, S.; Cioslowski, J.; Stefanov, B. B.; Liu, G.; Liashenko, A.; Piskorz, P.; Komaromi, I.; Martin, R. L.; Fox, D. J.; Keith, T.; Al-Laham, M. A.; Peng, C. Y.; Nanayakkara, A.; Challacombe, M.; Gill, P. M. W.; Johnson, B.; Chen, W.; Wong, M. W.; Gonzalez, C.; Pople, J. A. Gaussian 03, Revision B.05, Gaussian, Inc.: Pittsburgh, PA, 2003.

(19) (a) Becke, A. D. *J. Chem. Phys.* **1993**, *98*, 5648. (b) Lee, C.; Yang, W.; Parr, R. G. *Phys. Rev. B* **1988**, *37*, 785.

(20) (a) McLean, A. D.; Chandler, G. S. *J. Chem. Phys.* **1980**, *72*, 5639. (b) Krishnan, R.; Binkley, J. S.; Seeger, R.; Pople, J. A. *J. Chem. Phys.* **1980**, *72*, 650.

(21) Head-Gordon, M.; Pople, J. A.; Frisch, M. *Chem. Phys. Lett.* **1988**, *153*, 503.

(22) (a) Jacox, M. E. *Rev. Chem. Intermed.* **1978**, *2*, 1. (b) Jacox, M. E. In*Chemistry and Physics of Matrix Isolated Species*; Andrews, L.; Moskovits, M, Eds.; Elsevier Science Publishers B. V.: The Netherlands, 1989; p75.

(23) (a) Jacox, M. E.; Milligan, D. E. *J. Chem. Phys.* **1970**, *53*, 2688. (b) Jacox, M. E.; Milligan, D. E. *J. Chem. Phys.* **1967**, *47*, 1626.

(24) Andrews, L.; Smith, D. W. *J. Chem. Phys.* **1970**, *53*, 2956.

(25) Fridgen, T. D.; Zhang, X. K.; Parnis, J. M.; March, R. E. *J. Phys. Chem. A* **2000**, *104*, 3487.

(26) (a) Bondybey, V. E.; Pimentel, G. C. *J. Chem. Phys.* **1972**, *56*, 3832. (b) Milligan, D. E.; Jacox, M. E. *J. Mol. Spectrosc.* **1973**, *46*, 460. (c) Wight, C. A.; Ault, B. S.; Andrews, L. *J. Chem. Phys.* **1976**, *65*, 1244.

(27) (a) Chertihin, G. V.; Andrews, L. *J. Chem. Phys.* **1998**, *108*, 6404. (b) Thompson, W. E.; Jacox, M. E. *J. Chem. Phys.* **1989**, *91*, 3826. (c) Chertihin, G. V.; Saffel, W.; Yustein, J. T.; Andrews, L.; Neurock, M.; Ricca, A.; Bauschlicher, C. W. *J. Phys. Chem.* **1996**, *100*, 5261.

(28) (a) Milligan, D. E.; Jacox, M. E. *J. Chem. Phys.* **1963**, *38*, 2627. (b) Smith, D. W.; Andrews, L. *J. Chem. Phys.* **1974**, *60*, 81.

(29) (a) Zhou, H.; Gong, Y.; Zhou, M. F. *J. Phys. Chem. A* **2007**, *111*, 603. (b) Jalbout, A. F.; El-Nahas, A. M. *J. Mol. Struct. (THEOCHEM)* **2004**, *671*, 125.

(30) (a) Jacox, M. E.; Milligan, D. E. *J. Chem. Phys.* **1965**, *43*, 866. (b) Schnockel, H.; Eberlein, R. A.; Plitt, H. S. *J. Chem. Phys.* **1992**, *97*, 4. (c) Fridgen, T. D.; Parnis, J. M. *J. Phys. Chem. A* **1997**, *101*, 5117.

JP809683N